Development of Magnetic Latching Relay for Improvement of Tripping Current Variation Under Manufacturing Error

Takafumi Nakagawa

Abstract—**This paper proposes a magnetic latching relay with a permanent magnet to improve the tipping current variation in operation. We propose a new structure that adopts a partly saturated iron yoke and a thin non-magnetic plate on a contact surface. The magnetic structure is optimized by Taguchi's design methodology and FEM calculations. The variation of latching magnetic force is minimized and the current sensitivity is increased by evaluating the performance of operation curve under manufacturing error. The performance of the developed relay is studied in comparison to our conventional one with calculations and experiments. The developed relay decreases the tripping current variation to less than half that of the conventional one.**

Index Terms— **Magnetic latching relay, robust design, finite element method, Taguchi method**

I. Introduction

Many types of magnetic switches with a permanent magnet and a spring are widely used as triggers for trippers in breakers [1]-[7]. A plunger is magnetically latched by the magnetic flux generated by a permanent magnet. It compresses a spring when power is off. When the magnetic force becomes lower than the spring force, the plunger is launched. The tripping current varies due to manufacturing error. This leads to a variation of release timing or rising cost of providing an electric circuit. It is important subject to suppress this variation in mass production. There are some works which have improved the response time by optimization of magnetic structures [8]-[13]. However, these works did not discuss the variation of the tripping current or release timing. As for optimization techniques, stochastic methods using a genetic algorithm or simulated annealing algorithm have been widely used to find optimal structure [14]-[18]. The orthogonal array method [19] [20] or the response surface method have also been used to decide the magnetic structure at low cost [21] [22]. However, these works did not consider the performance variations generated by the manufacturing error. Therefore, if a solution obtained by these optimization techniques is very sensitive to small perturbation, it will not be of practical use. That is, lack of reproducibility may occur in the field when the product performance is highly dependent on tight control of the design parameters or the interactions among them. In comparison with these techniques, robust design aims at achieving not only the expected performance but also reproducibility of the performance in the field. The Taguchi method has been widely used as a robust design technique for magnetic circuit designs [23]-[29]. This method calculates the cause-and-effect between the parameters and the performance in a few experimental runs, and finds the parameters that produce the main effect on the performance. The key point in using Taguchi's approach is to find a good additive model of controllable factors instead of measuring quality performance. The additive model is defined as a function to describe the expected performance in a system. The degree of deviation from the expected function is evaluated with the SN ratio. Many additive models are used in Taguchi's design methodology. For instance, the proportional relation between the magnetic force and coil current was evaluated to stabilize magnetic thrust force in a linear actuator, and the magnetic structure was optimized with response curve [27]. The locomotion of a lens proportional to the driving force was used in the position pickup system, and its structure was optimized under the production errors [28]. In a solenoid relay, the time variation of tripping current was investigated, and the electric circuit was optimized to shorten response time [3]. To improve the magnetic force distribution in a solenoid actuator, the linear relationship between the magnetic force and gap length on a contact surface was evaluated, and the shape of the plunger was refined [29]. In a magnetic actuator used in the circuit breaker, the trajectory of the electrical contact was evaluated under the variation of electric components, and the electric circuit was stabilized [30]. As for an actuator driving compressor, Lorentz force was evaluated under variations of air gaps along a coil guide [31]. However, these past works did not give solutions for improvement of the tripping current variation under the manufacturing error.

In this paper, we develop a magnetic latching relay to improve the variation of tripping current. The magnetic structure is optimized by Taguchi's design methodology and FEM calculations. The magnetic structure is optimized to decrease the variation of magnetic force when the power is off and the sensitivity increased in operation. The performance of this relay is studied by calculations and experiments in comparisons with our conventional one.

Takafumi Nakagawa is with Advanced Technology R&D Center, Mitsubishi Electric Corporation, 8-1-1, Tsukaguchi-Honmachi, Amagasaki, Hyogo, JAPAN (corresponding author to provide phone: +81-06-6497-7245;fax:+81-06-6497-7288;e-mail:Nakagawa.Takafumi@dr.MitsubishiElectric.co.jp).

II. DEVELOPED MAGNETIC LATCHING RELAY

The outline of the developed relay is shown in Fig. 1 (a), and its cross section is illustrated in Fig. 1 (b). This relay includes a ring-shaped permanent magnet, a solenoid coil, a cylindrical plunger and a spring. The plunger is surrounded by a C-shaped outer yoke and a bridging plate. The bridging plate has a cylindrical opening to insert a plunger. A baseplate is installed between the plunger and an outer yoke. A thin non-magnetic plate is put on the baseplate. In Fig. 1 (b), the solid-arrow lines show the magnetic flux generated by the permanent magnet. The dotted-arrow lines show the magnetic flux generated by a coil. The plunger is magnetically latched on the baseplate, and it suppresses a spring with a spring plate when power is off. The strength of latching force can be controlled by the size of a window made on the outer yoke. A larger window produces stronger force while the tripping current is increased. The symbols from A to F in Fig. 1 (b) show the factors to control the performance. The distribution of the magnetic flux when power is off is shown in Fig. 2, which is calculated with the 1/4 model. From Fig. 2 (b), both sides of the window are magnetically saturated to reduce the variation of magnetic flux in manufacture. The relationship between the magnetic force and coil currents in operation is illustrated in Fig. 3. The solid line shows a nominal operation curve, and the dotted lines are deviations from the nominal operation under two noise conditions such as manufacturing error. A two-dot chain line shows repulsion force by a spring. When the coil is excited and the magnetic force becomes smaller than the spring force, the plunger is released. The tripping current varies depending on the difference between the magnetic latching force and the spring force. In addition, good sensitivity is required to operate with low power consumption. The sensitivity corresponds to a slope of the operation curve in Fig. 3. A relay with larger sensitivity works on lower power. Figure 4 shows the comparison of calculations and experiments in our conventional relay. The magnetic force on the baseplate is calculated by FEM calculation and compared with the measurements. The magnetic force is normalized by the maximum force. The solid curve gives the measurements, and black circles are calculations. These calculations agree with measured values. The magnetic force decreases to 85 % of the maximum value at the gap length of 0.01 mm. Figure 5 shows a comparison with calculations and measurements of operation curve in our conventional relay. The white circles give the calculations, and black circles are measurements. These calculations are in good agreement with the measurements. The magnetic force decreases in proportion to the coil current until reaching the repulsion force.

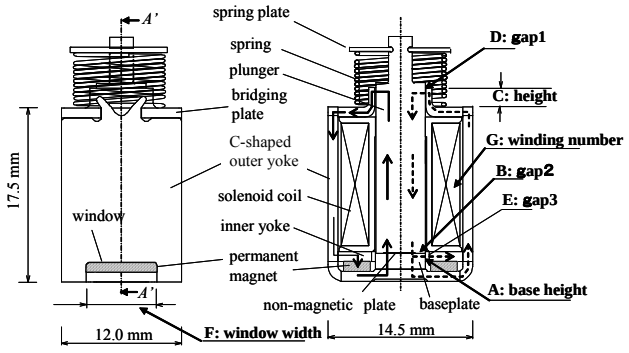

(a) Outline of magnetic latching relay (b) Cross section along A'-A'

Fig. 1. Structure of developed relay. The solid-arrow lines show the magnetic flux generated by the permanent magnet. The dotted-arrow lines show the magnetic flux generated by a coil.

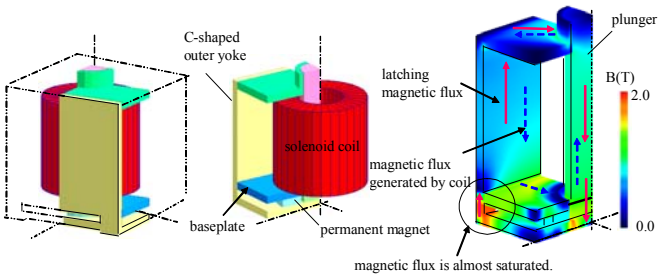

(a) Calculation model (b) Magnetic flux distribution

Fig. 2. 1/4 model and calculated distribution of magnetic flux when power is off.

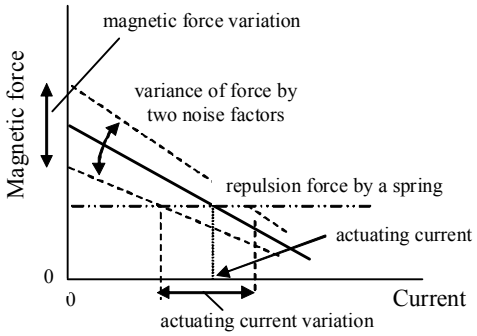

Fig. 3. Illustrated operation curve under two noise factors. A solid line shows a nominal operation curve and the dotted lines are deviations from the nominal operation under two noise conditions. A two-dot chain line shows the repulsion force by a spring.

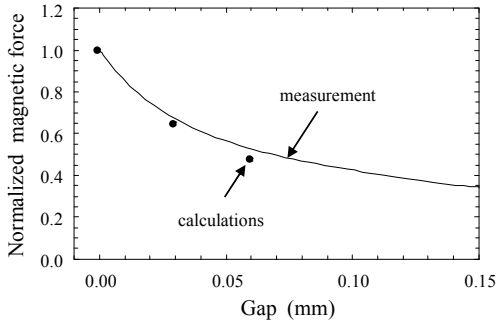

Fig. 4. Comparison of calculations and experiments in our conventional relay. The magnetic force is normalized by the maximum force.

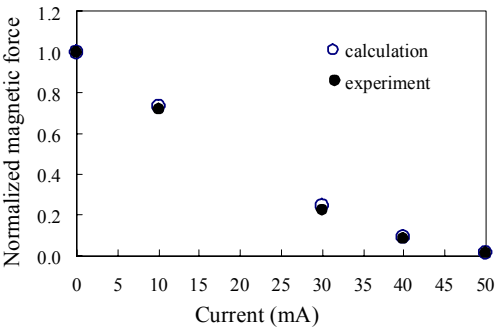

Fig. 5. Comparison of calculations and measurements of magnetic force against coil current in our conventional relay. The magnetic force is normalized by the maximum force.

III. ROBUST DESIGN

The following SN ratio is used to evaluate the degree of variation of the operation curve under noise conditions. SN ratio and sensitivity are calculated by the following equations [23] [32]. The relationship between signal and response is approximated by a straight line $y_{ij}=\beta_i M_j$, where β_i represents a slope in each experimental run with orthogonal array (OA). M_j is a signal and y_{ij} is a response.

$$SN = 10\log_{10}\left(\overline{\beta}^2/\sigma^2\right),\ Sensitivity = 10\log_{10}\left(\overline{\beta}^2\right) \quad (1)$$

$$\overline{\beta} = \sum\nolimits_j \beta_j / q \quad (2)$$

$$y_{ij} = \beta_j M^*{}_i + e_{ij}, i = 1,\cdots,p; j = 1,\cdots,q \quad (3)$$

$$M_i^* = \sum\nolimits_j y_{ij} / q \quad (4)$$

where $M^*{}_i$ is the averaged output signal, and e_{ij} is the regression error. j refers to the experimental runs in OA. i refers to the number of input signals. The total mean square error from the regression line is given by

$$\sigma^2 = \frac{\sum_{j=1}^{k}\sum_{i=1}^{n}((\beta_j-\overline{\beta})*M^*{}_i)^2 + \sum_{j=1}^{k}\sum_{i=1}^{n}(y_{ij}-\beta_j M^*{}_i)^2}{(pq-1)*q*\sum_i M^{*2}{}_i} \quad (5)$$

where p and q show the number of input signal and experimental run. The larger SN ratio gives the smaller variation in the response. In the first step, the optimal setting of the controllable factors is determined to increase the SN ratio. In the second step, the other factors are used to improve the magnetic sensitivity to the operating current. Figure 6 shows an example of the calculated relationship between averaged magnetic force and operating magnetic force under two noise conditions, noise 1 and noise 2. A slope of a regression line is equal to 1 when the operating force coincides with the averaged force under two noises.

A. Identifying Noise and Control Factors

The eight kinds of noise factors and their levels are presented in Table I. Symbol A is remnant magnetization Br of a permanent magnet. Symbol B is gap length on a baseplate, which is decided by coating thickness, and symbol C is diameter of a plunger. Symbol D is gap length between a plunger and a bridging plate, and E is gap length between a baseplate and an inner yoke. Symbol F is window width on the outer yoke. Symbol G shows winding number, and symbol H is diameter of a permanent magnet. The three kinds of levels are sets for each factor except symbol A. The column of Level 2 indicates the nominal values. The levels of A are determined in view of the temperature rises. The other levels except for symbol G are decided from the manufacturing tolerance. These factors are assigned to OA of L18 ($2^1\times3^7$).

At first, a change of the operation curve is calculated with OA. The response curve is plotted in Fig. 7. The horizontal line shows the kinds of noise factors. The vertical lines show the magnetic sensitivity in operation and the magnetic force when the power is off. These data are normalized by the averaged value. This figure shows that factors B, D and H have strong effects on change of the magnetic force. In other words, the magnetic force is increased with the larger magnetic flux and smaller gap. As for the sensitivity, the impact factors are B, D, G and H. These factors give similar tendency to sensitivity as magnetic force. Factor B strongly affects both performances. From these results, the eight noise factors are compounded to two additional noises to reduce the computation cost in the following calculations. These compounded factors are listed in Table II. Factor F is omitted because the manufacturing tolerance does not affect the change of magnetic force.

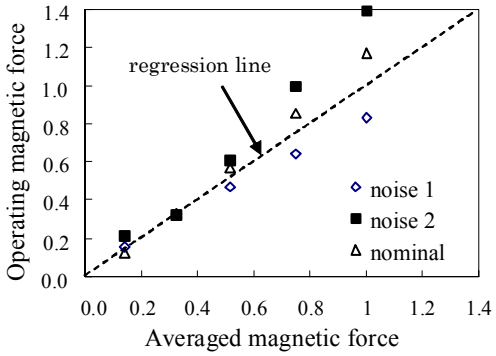

Fig. 6. Example of the calculated relationship between averaged magnetic force and operating magnetic force under two noise conditions: noise 1 and noise 2.

TABLE I
COMPOUNDED NOISE FACTOR

Symbol		detail	Level 1	Level 2	Level 3
A	T	remnant magnetization Br	1.03	1.11	-
B	mm	gap length of gap2	0.016	nominal	-0.016
C	mm	diameter of a plunger	0.05	nominal	-0.05
D	mm	gap length of gap1	0.05	nominal	-0.05
E	mm	gap length of gap3	0.05	nominal	-0.05
F	mm	window width	0.10	nominal	-0.10
G	%	winding number	-30.0	nominal	+30.0
H	mm	diameter of a permanent magnet	-0.20	nominal	0.20

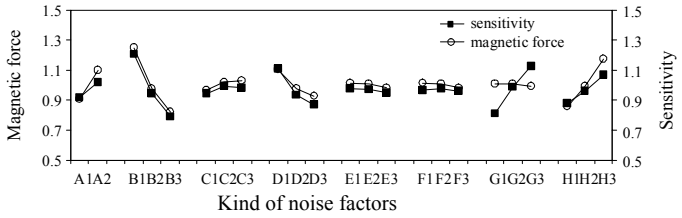

Fig. 7. Response curve for noise factors. The horizontal line shows the kinds of noise factors. The vertical lines show the magnetic sensitivity in operation and the magnetic force when the power is off. These data are normalized by the averaged value.

TABLE II
COMPOUNDED NOISE FACTORS

Symbol		detail	N1	N2
A	T	remnant magnetization Br	1.03	1.11
B	mm	gap length of gap2	0.016	-0.016
C	mm	diameter of a plunger	0.05	-0.05
D	mm	gap length of gap1	0.05	-0.05
E	mm	gap length of gap3	0.05	-0.05
F	%	winding number	-30.0	+30.0
G	mm	diameter of a magnet	-0.2	0.2

In the next step, the controllable factors mainly affecting the operation curve are investigated under the compound noise conditions. The controllable factors are listed in Table III, and these factors are illustrated in Fig. 1. Seven kinds of control factors are selected: height of a baseplate, three kinds of gap length, height of a cylindrical opening on a bridging plate, window width on an outer yoke, and winding number. The OA of L18 ($6^1 \times 3^6$) is adopted to accommodate factor A including six levels.

TABLE III
CONTROLLABLE FACTORS

Symbol		detail	Level 1	Level 2	Level 3	Level 4	Level 5	Level 6
A	mm	height of basplate	0.0	1.0	1.5	2.0	2.5	3.0
B	mm	length of gap2	0.02	0.08	0.12			
C	mm	height of a cylindrical opening	0.0	1.5	3.0			
D	mm	length of gap1	0.1	0.2	0.4			
E	mm	length of gap3	0.1	0.2	0.4			
F	mm	window width	9.0	7.0	5.0			
G	%	winding number	-20.0	nominal	+20.0			

B. Calculated Results

The calculated SN ratio and magnetic sensitivity for controllable factors are summarized in Table IV. Numbers from 1 to 6 show the levels of controllable factors shown in Table III. Figure 8 shows the calculated response curve. The white circles and black squares show the SN ratio and the sensitivity, respectively. Figure 9 shows contributing rate calculated by factor analysis. The slashed and shaded columns show the SN ratio and sensitivity. From these figures, the factors of A, B, D, E and F have significant effects on the SN ratio. In other words, the height of the baseplate and three kinds of gap length dominate the change of the magnetic force. This means that the higher baseplate leads to saturating the magnetic flux on the contact surface and improving the change of the magnetic force. From Fig.8, the three kinds of gap length show a trade-off between the SN ratio and sensitivity. The larger window also leads to suppressing the change of the magnetic force. The factors of C and G can increase the sensitivity without decreasing the SN ratio.

TABLE IV
CALCULATED SN RATIO AND MAGNETOC SENSITIVITY

Experiment No.	Controllable factors A	B	C	D	E	F	G	SN (db)	Sensitivity (db)
1	1	1	1	1	1	1	1	3.6	-13.1
2	1	2	2	2	2	2	2	11.2	-9.7
3	1	3	3	3	3	3	3	17.7	-13.3
4	2	1	1	2	2	3	3	8.1	-6.7
5	2	2	2	3	3	1	1	10.8	-12.0
6	2	3	3	1	1	2	2	15.4	-11.9
7	3	1	2	1	3	2	3	9.5	-2.7
8	3	2	3	2	1	3	1	24.3	-15.7
9	3	3	1	3	2	1	2	20.5	-15.7
10	4	1	3	3	2	2	1	17.6	-9.0
11	4	2	1	1	3	3	2	19.7	-11.7
12	4	3	2	2	1	1	3	28.9	-20.0
13	5	1	2	3	1	3	2	28.5	-17.3
14	5	2	3	1	2	1	3	23.4	-8.9
15	5	3	1	2	3	2	1	23.2	-16.9
16	6	1	3	2	3	1	2	14.3	-6.2
17	6	2	1	3	1	2	3	32.1	-24.0
18	6	3	2	1	2	3	1	29.5	-17.8

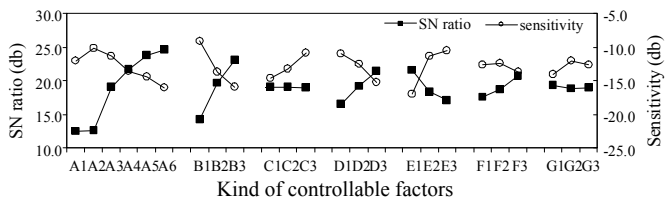

Fig. 8. Calculated response curve for controllable factors. The white circles and black squares show the SN ratio and magnetic sensitivity, respectively. The dashed lines represent mean values.

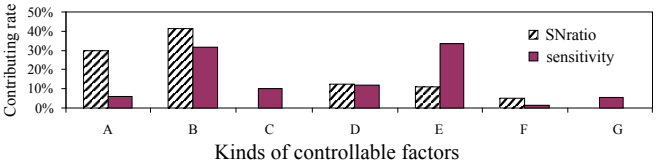

Fig. 9. Contributing rate of controllable factors in the factor analysis. The slashed and shaded columns show the SN ratio and sensitivity.

C. Confirmation Test of Parameters

A confirmation test is usually required to remove concerns about the choice of parameters because the additive effectiveness by controllable factors is supposed in the Taguchi method. The predicted changes with the additive model are compared with calculations by FEM calculation. The following parameter sets of Model 1 and Model 2 are selected as the confirmation tests. Their parameters and levels are A4, B2, C3, D3, E1, F2, G2 for Model 1, and A1, B1, C1, D1, E1, F2, G2 for Model 2. Factors A and B mainly influence the latching force. The variations of operation curves for both models are investigated under the compound noise conditions. The result of the confirmation test is summarized in Table V. "Prediction" is calculated from the additive effectiveness of the response curve plotted in Fig. 8. "Calculation" shows the calculated result by FEM calculation. The predicted "Gain", which refers to the difference between Model 1 and Model 2, are 10.5 db for the SN ratio and 1.5 db for the sensitivity. In contrast, the calculated gains are 9.0 db for the SN ratio and 1.3 db for the sensitivity. The predicted gains are almost the same as the calculated gains. This means that the selected factors of A, B, C and D give the additive effectiveness. We have conclusively selected the factors of A3, B2, C3, D1, E2, F1 and G2 in considering the specification of magnetic latching force.

TABLE V
RESULTS OF CONFIRMATION TEST

Model	SN ratio (db)		Sensitivity (db)	
	Prediction	Calculation	Prediction	Calculation
Model1	17.6	16.6	-8.1	-6.4
Model2	7.2	7.6	-9.6	-7.7
Gain	10.5	9.0	1.5	1.3

IV. RESULTS AND DISCUSSION

The validity of this design was studied by calculations and experiments. Figure 10 shows the calculated relationship of magnetic force and tripping current between the developed relay and the conventional one. The solid line and dotted line show operation curve of the developed relay and the

conventional one, respectively. The symbols N1 and N2 refer to the calculations under the compounded noise conditions shown in Table II. The magnetic force is normalized by the nominal values when power is off. ΔF and Δi show the possible fluctuating ranges of the magnetic force when power is off and the variation of tripping current in operation. The suffix "cov" and "dev" refer to the value of the conventional relay and the develop one, respectively. It is expected that the developed relay can reduce these variances to about half ($=\Delta F_{dev}/\Delta F_{cov}$) and one-third ($=\Delta i_{dev}/\Delta i_{cov}$) of the conventional one. The change of magnetic latching force has a significant effect on the tripping current variations. Therefore, to reduce the tripping current variations, it is effective to make the change of the magnetic force smaller as possible. For this reasons, we propose a new structure that adopts a partly saturate iron yoke and a non-magnetic plate on a contact surface.

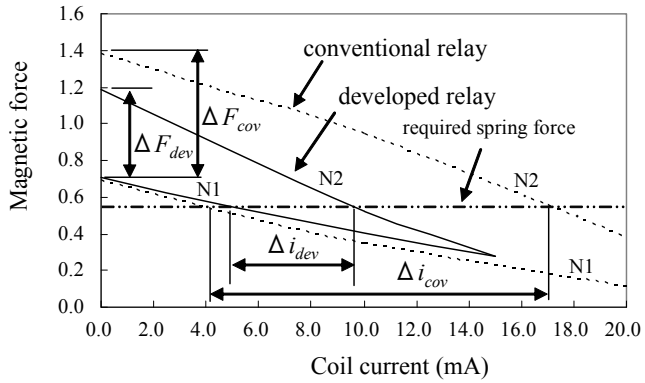

Fig. 10. Calculated relationship of magnetic force and tripping current between the developed relay and the conventional one. The lines with symbols N1 and N2 refer to the calculations under the compounded noise conditions. The magnetic latching force is normalized by the nominal values when power is off.

To confirm the performance of the developed relay, two relays were produced experimentally. The measured performance of the developed relays is shown in Table VI. From Table VI, the sensitivity is almost proportional to ampere-turn. The latching magnetic force is 7.07 and 7.22 N for relay No.1 and No.2 when power is off. The static friction is 0.3 N which is determined by the plunger and coil bobbin. From the magnetic sensitivity shown in Table VI, if a change of latching magnetic force of 0.15 N occurs, it leads to the change of tripping current of 0.8 mA and 0.4 mA in relay No.1 and No.2.

TABLE VI
MEASURED PERFORMANCE OF DEVELOPED RELAYS

relay No.	1	2
winding (turn number)	4700	8500
R (Ω)	606	2140
latching magnetic force(N)	7.07	7.22
friction (N)	0.31	0.30
magnetic sensitivity (N/mA)	0.18	0.37
tripping current (mA)	12.03	6.86
spring force (N)	4.5	

Figure 11 shows the measured magnetic force against the gap length on the baseplate. The solid line shows the developed relay, and the dotted line refers to the conventional one. The magnetic force of the developed relay is measured in two cases, with a non-magnetic plate of 0.08 mm thickness and without one. The magnetic force is normalized by the maximum value. From Fig. 11, the measured magnetic force decreases very steeply in the conventional relay. In contrast, it gradually changes in the developed relay. The magnetic latching force in the developed relay decreases to only about 3 % of maximum value at the gap length of 0.01 mm. However, it is about 15 % in the conventional one. Therefore, the conventional relay is relatively sensitive to the gap length while the developed relay has low sensitivity The non-magnetic plate of 0.08 mm thickness is selected to ensure the smaller change of magnetic force.

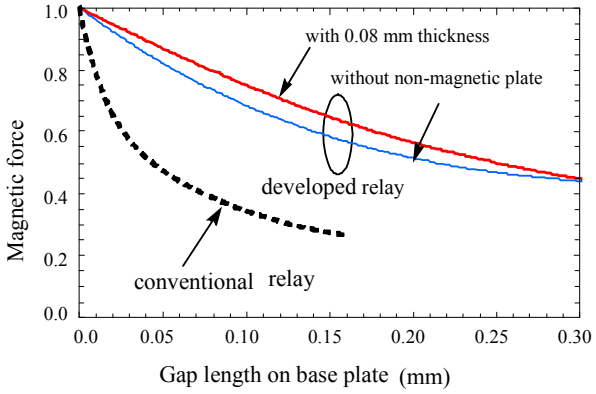

Fig. 11. Measured magnetic force against the gap length on the baseplate. The magnetic force of the developed relay is measured in two cases

Figure 12 shows the measured operation curves. The solid line and the dotted lines refer to the developed relay and the conventional one. The ampere-turn in the developed relay is converted to the same as that of the conventional one. The magnetic force is normalized by the maximum force. The sensitivity of the developed relay is almost equivalent to the conventional one.

From the above studies, it is expected that the variation of tripping current in the developed relay will be smaller than the conventional one.

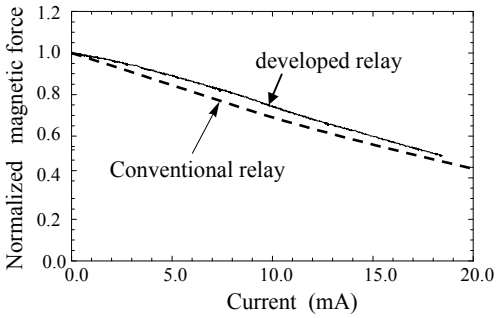

Fig. 12. Measured operation curves. The solid line and the dotted lines show the developed relay and the conventional one. The magnetic force is normalized by the maximum force.

To confirm the validity of this design, the tripping current of relay was measured with four kinds of springs in a same relay No.1. It is well known the variation of spring force and friction affects on the tripping current variation. Ten measurements were done for each spring. Fig.13 shows the comparison of tripping current between the developed relay

and the conventional one. The horizontal line shows spring number, and the vertical lines show the tripping current normalized by averaged current. The comparison of the measured tripping current is summarized in Table VII. "Max (cur)" and "Min (cur)" show maximum and minimum values among averaged currents. "Max variation" denotes the difference between the "Max (cur)" and "Min (cur)". σ shows the averaged mean square deviation for each measurement. From Table VII, the maximum variation of tripping current was 32% for the conventional relay and 11% for the developed one. Hence, the current variation in the developed relay is smaller than that in the conventional one.

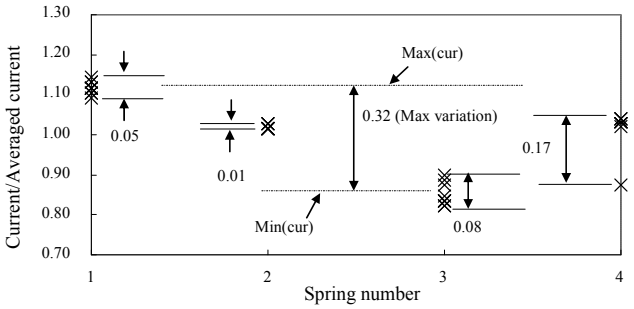

(a) Variation of tripping current in our conventional relay

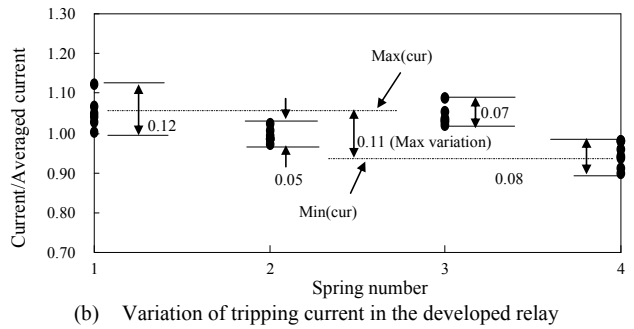

(b) Variation of tripping current in the developed relay

Fig. 13. Comparison of tripping current between the developed relay and the conventional one. Fig. 13 (a) and (b) show the measurements of the conventional relay and the developed one, respectively. The horizontal line shows the number of the spring, and the vertical lines show the tripping current, which was normalized by averaged current.

This reason is as follows. The structure of a conventional relay and the distribution of magnetic flux density are illustrated in Fig. 14. The magnetic flux distribution is calculated by 1/4 model when power is off. The dotted-arrow line shows the magnetic flux generated by a coil and the solid line shows the magnetic flux generated by the permanent magnet. The magnetic flux generated by the permanent magnet is saturated at the contact surface. The magnetic sensitivity is affected by the degree of this saturation and the gap length between a baseplate and C-shaped outer yoke. This gap length varies due to staking of a baseplate on the permanent magnet and the outer yoke. This structure also

TABLE VII
COMPARISON OF MEASURED TRIPPING CURRENT

	Developed Relay	Conventional Relay
Max (cur)	1.05	1.14
Min (cur)	0.94	0.82
Max variation	0.11	0.32
σ	0.05	0.10

produces the variation of gap length on the contact surface by tilting movement of a plunger because the plunger directly contact on the baseplate. Therefore, these variations make the variation of magnetic force and sensitivity. The conventional relay is also relatively sensitive to the gap on the contact surface as shown in Fig. 11. For theses reasons, the tripping current variation becomes larger than the developed one.

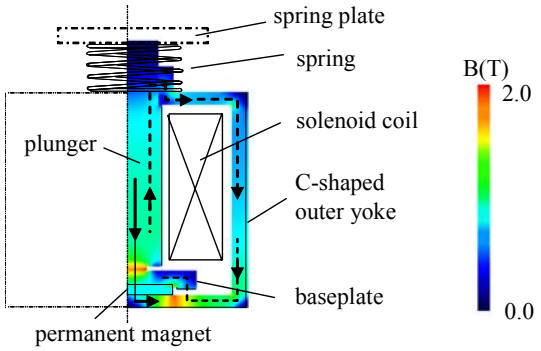

Fig. 14. Illustrated structure and distribution of magnetic flux density in a conventional relay. The magnetic flux distribution is calculated with 1/4 model. The solid-arrow lines show the magnetic flux generated by a permanent magnet. The dotted-arrow lines show the magnetic flux

Figure 15 shows the measurements of latching force of relay No.1 against coil current without a spring. The sensitivity gradually increases depending on current while latching force linearly decreases.

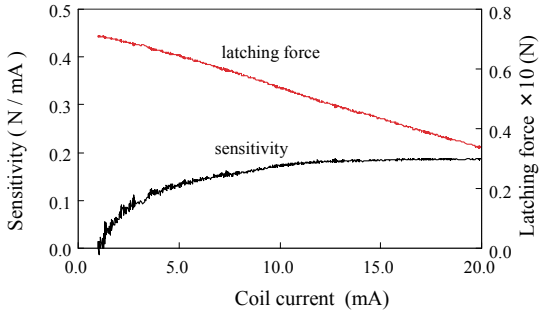

Fig. 15. Change of latching force and sensitivity against tripping current.

The measured dynamic characteristic of relay No.1 is shown in Fig. 16. The releasing time was about 2.0 msec when the spring force was 4.5 N. The tripping current was 14.7 mA. The current variation is calculated as follows. In the developed relays, the tripping current variation is mainly determined by the change of magnetic latching force, spring force and friction. The variation of magnetic force is produced by the change of gap length on the baseplate. This change of gap length is also produced by the tilt of the plunger during repetitive motion. But it is structurally small because the clearance between the spring plate and plunger is very large. As for the variation of a permanent magnet, the measured remnant magnetization was below 1%, which was also negligible change. The change of latching magnetic force caused by coating thickness was also presumed to be about 0.25 N from Table I and Fig. 11. This change gives current variation of 1.4 mA. The measured variation of the spring force was 0.25 N within 3σ; thus, this makes the current variation of 1.4 mA. When we also assumed the

change of friction as Fr N, the current variation increased Fr/0.18 mA in addition. Therefore, the total variation leads to ± (2.8+Fr/0.18) mA. The sensitivity is almost proportional to ampere-turn. Therefore, although the releasing time leads to longer, tripping current variation decreases by increasing ampere-turn of a coil.

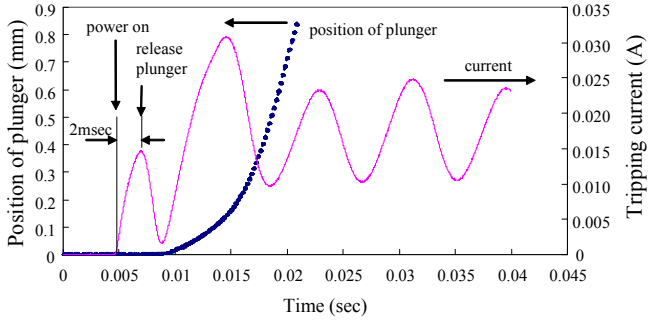

Fig. 16. Measured dynamic characteristics of the developed relay No.1.

V. Conclusion

A magnetic latching relay was developed to improve the variation of tripping current under the manufacturing error. The change of magnetic force caused by the manufacturing error was improved by developing a new structure that adopts a partly saturated iron yoke and a thin non-magnetic plate installed on the contact surface. The magnetic structure was designed using Taguchi's design methodology and FEM calculations. The variation of latching magnetic force was minimized and the current sensitivity was increased at the same time by evaluating the performance of operation curve under the manufacturing error. The validity of this design methodology was confirmed by experiments through comparisons with our conventional relays. In consequence of this design, the measured variation decreased to less than half that of our conventional one.

Acknowledgment

The author is grateful to Mr. Y. Sugimoto and Dr. Y. Makita, and also wishes to thank Dr. K. Haruna for many valuable comments and suggestions.

References

[1] Y. Makita, T. Nakagawa, K. Haruna, Y. Sugimoto, "Design Technologies of Electromagnetic Relay Using Taguchi Method for MCCB and ELCB of WS-V Series," *Mitsubishi Denki Giho*, vol.84, no.2, pp.131-134, 2010 (In Japanese)

[2] T. Kudo, M.Wada, S.Sugiyama, Y.Takahashi, H.Asano and M.Mitsushige, "Dynamic Response Simple Analysis of a Capacitance-Drive –Type Linear Electromagnetic Solenoid", *Journal of the Magnetics Society of Japan*, vol.29, no.1, pp.41-46, 2005 (Japanese)

[3] T.Kudo, Y.Takahashi, I.Takamatsu and S.Wakui, "A Robust Design of Capacitance-Drive-Type Linear Electromagnetic Solenoid", *Journal of the Magnetics Society of Japan*, vol.30, no.3, pp. 413-417 ,2006 (In Japanese)

[4] L. Erping, P. M. McEwan, "Analysis of a circuit breaker solenoid actuator system using the decoupled CAD-FE-integral technique," *IEEE Transactions on Magnetics*, vol. 28, no.2, pp.1279-1282, 1992

[5] J. Sato, 0. Sakaguchi, N. Kubota, S. Makishima, S. Kinoshita, T. Shioiri, T. Yoshida, M. Miyagawa, M. Homma. and E. Kaneko, "New technology for medium voltage solid insulated switchgear," *Transmission and Distribution Conference and Exhibition 2002: Asia Pacific. IEEE/PES*, vol.3, pp.1791-1796, 2002

[6] L. Xin, G. Huijun and C. Zhiyuan, "Magnetic field calculation and dynamic behavior analyses of the permanent magnetic actuator," *XIXth International Symposium on Discharges and Electrical Insulation in Vacuum: ISDEIV 2000*, vol.2, pp.532-535, 2000

[7] H. Jiang, R. Shuttleworth, B.A.T. AI Zahawi, "Variable speed latching magnetic actuator for a vacuum switch," *Eighth International Conference on Electrical Machines and Drives*, pp.105-108, 1997

[8] M. Piron, P. Sangha , T. J. E. Miller, D. M. Ionel and J. R. Coles, "Rapid computer-aided design method for fast-acting solenoid actuators," *IEEE Transactions on Applications*, vol. 35, no.5, pp.991-999, 1999

[9] J. Kim and D.K. Lieu, "Designs for a new, quick-response, latching electromagnetic valve," *IEEE International Conference on Electric Machines and Drives*, pp.1773 – 1779, 2005

[10] Z. Li, B.R.Varlow, L.A.Renforth, D.W.Auckland and R.Shuttleworth, "Optimal design of autorecloser electromagnetic actuator," *IEE Proceedings - Electric Power Applications*, vol.147, no.5, pp.431-435, 2000

[11] B.J. Sung and E. W. Lee, "Optimal design of high-speed solenoid actuator using a non-magnetic ring," Proceedings of the *Eighth International Conference on Electrical Machines and Systems, ICEMS 2005*, vol.3, pp.2333-2338, 2005

[12] B.J. Sung, "A Design Method and Reliability Assessment of High Speed Solenoid Actuator," *Journal of International Council on Electrical Engineering*, vol.2, no.1, pp.110-118, 2012

[13] B.J. Sung, E.W. Lee, and Jae-Gyu Lee, "A design method of solenoid actuator using empirical design coefficients and optimization technique," *IEMDC '07. IEEE International Electric Machines and Drives Conference,* pp. 279 - 284, 2007

[14] P. G. Alotto, C. Eranda, B. Brandst¨atter, G. F¨urntratt, C. Magele, G. Molinari, M. Nervi, K. Preis and M. Repetto, "Stochastic Algorithms in Electromagnetic Optimization, " *IEEE Transactions on Magnetics,* vol. 34, no.5, pp.3674-3684, 1998

[15] J Simkin and C.W. Trowbridge, "Optimizing Electromagnetic devices combining direct search methods with simulated annealing," *IEEE Transactions on Magnetics*, vol.28, no.2, pp.1545-1548, 1992

[16] H. Enomoto, K. Harada, Y. Ishihara, T. Todaka and K. Hirata, "Optimal Design of Linear Oscillatory Actuator Using Genetic Algorithm," *IEEE Transactions on Magnetics*, vol.34, no.5, pp.3515-3518, 1998

[17] H. T. Wang, Z. J. Liu, T. S. Low, S. S. Ge, and C. Bi, "A Genetic Algorithm Combined with Finite Element Method for Robust Design of Actuators," *IEEE Transactions on Magnetics*, vol.36, no.4, pp. 1128 - 1131, 2000

[18] J. Maridor, M. Markovic, Y. Perriard and D. Ladas, "Optimization design of a linear actuator using a genetic algorithm," *IEMDC '09. IEEE International Electric Machines and Drives Conference*, pp. 1776 - 1781, 2009

[19] B. Zhang, J. Ma, L. Pan, X. Cheng and Y. Tang, "High performance three-axis actuator in super-multi optical pickup with low crosstalk force," *IEEE Transactions on Consumer Electronics*, vol.54, no.4, pp. 1743-1749, 2008

[20] H. Fusayasu, Y. Yokota, Y. Iwata and H. Inoue, "Optimization of a magnetic actuator with Taguchi Method and multivariate analysis method," *IEEE Transactions on Magnetics*, vol.34, no.4, pp. 2138-2140, 1998

[21] S. Brisset, F. Gillon, S. Vivier and P.l. Brochet, "Optimization with experimental design: an approach using Taguchi's methodology and finite element simulations," *IEEE Transactions on Magnetics*, vol.37, no.5, pp. 3530- 3533, 2001

[22] L.El Amraoui, F. Gillon, S. Vivier and P. Brochet, "Robust Electromagnetic Optimization of Linear Tubular Actuators," *IEEE Transactions on Magnetics*, vol.40, no.2, pp.1192-1195, 2000

[23] R. K. Roy, "Design of Experiments Using the Taguchi Approach," *Wiley-Interscience Publication*, 2001

[24] I.H. Choi, W.E. Chung, Y.J. Kim, I.S. Eom, H.M. Park and J.Y. Kim, "Compact Disk /Digital Video Disk (CD/DVD)-Compatible Optical Pickup Actuator for High Density and High Speed," *Jpn. J. Appl. Phys*, vol.37, pp.2189-2196, 1998

[25] A. Omekanda, "Robust Torque and Torque-per-Inertia Optimization of a Switched Reluctance Motor Using the Taguchi Methods," *IEEE Transactions on Industry Applications*, vol.42, no.2, pp.473-478, 2006

[26] T.S. Low, "Robust Torque Optimization for BLDC Spindle Motors," *IEEE Transactions on Industry Electronics*, vol.48, no.3, pp.656-663, 2001

[27] I. Yoshitaka, A. Yashushi, K. Hirata, H. Yabuuchi and T. Kunita, "Linear Oscillating Actuator with a Built-in Dynamic Vibration Absorber, " *Panasonic Electric Works Technical Report*, pp.75-82, 2001 (In Japanese)

[28] H. Nagasawa, H. Aso and N. Miyagi, "Optimizing the Design of Lens Driving Actuators for Optical Pickups," *Konica Minolta Technical Report*, vol.3, pp.68-71, 2006 (In Japanese)
[29] M. Abe, Y. Yamamoto, H. Kawanishi and T. Sako, "Improvement of a plunger type solenoid's robustness," *Isuzu Denki Giho*, nol.15, pp.49-54, 2006 (In Japanese)
[30] K. Imamura, T. Maeda and Y. Yamachi, "Robust design of vacuum circuit breaker aimed for restraint chattering," *QES 16*, pp.538-541, 2008 (In Japanese)
[31] J. Hee Kim, J. Hyung Kim and J.Ho Kim, "Robust Design of Air Compressor-Driving Quadratic Linear Actuator in Fuel Cell BOP System using Taguchi Method," *ISSN Journal of Magnetics,* pp.275-279, 2012
[32] T. Nakagawa, and T. Kirikoshi, "Robust Parameter Design Methodology for Microwave Circuits Considering the Manufacturing Variations," *IAENG International Journal of Computer Science*, vol.39 issue 2, pp.214-219, 2012